Corruptive Artifacts Suppression for Example-Based Color Transfer

Zhuo Su, *Student Member, IEEE*, Kun Zeng, Li Liu, Bo Li, and Xiaonan Luo

***Abstract*—Example-based color transfer is a critical operation in image editing but easily suffers from some corruptive artifacts in the mapping process. In this paper, we propose a novel unified color transfer framework with corruptive artifacts suppression, which performs iterative probabilistic color mapping with self-learning filtering scheme and multiscale detail manipulation scheme in minimizing the normalized Kullback-Leibler distance. First, an iterative probabilistic color mapping is applied to construct the mapping relationship between the reference and target images. Then, a self-learning filtering scheme is applied into the transfer process to prevent from artifacts and extract details. The transferred output and the extracted multi-levels details are integrated by the measurement minimization to yield the final result. Our framework achieves a sound grain suppression, color fidelity and detail appearance seamlessly. For demonstration, a series of objective and subjective measurements are used to evaluate the quality in color transfer. Finally, a few extended applications are implemented to show the applicability of this framework.**

***Index Terms*—Color transfer, computational photograph, edge-preserving smoothing, image manipulation.**

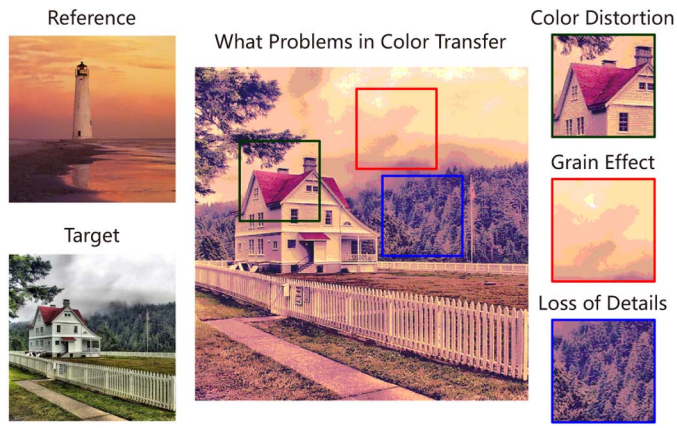

Fig. 1. Example-based color transfer [7] is an intuitional image manipulation technique, but it would produce some unexpected artifacts due to the complexity of color mapping. Grain effect, color distortion and loss of details appear in the transferred result commonly.

I. Introduction

COLOR manipulation is one of the most common tasks in image editing. While artists resort to photo editing tools to manually adjust color appearance, automatic color appearance adjustment is still of high demand, owing to the inherent difficulties to handle complex structures ubiquitous in natural images. Arguably, example-based color transfer [1], which aims at copying the color appearance from a given "example" to a target grayscale or color image, is the most effective way to tackle the problem. Rapid development has been witnessed in the last decade in the field of color transfer. Representative approaches include classical histogram matching, statistical transfer [2], N-dimensional probability density function transfer [3], gradient-preserving transfer [4], non-rigid dense correspondence transfer [5], progressive transfer [6], to list a few.

Although these approaches are effective in transferring the color information, they would occasionally produce visual artifacts, owing primarily to the contradictive roles of color distribution preservation and image content distribution. Taking Fig. 1 as an example, due to the big difference in the intensity distribution between the reference and the target, an unsatisfactory transferred result was produced, with remarkable artifacts as follows.

Color distortion. Some disharmonious or unexpected colors appear which are not included in the reference image.

Grain effect. A phenomenon appears due to enhancing the noise level of the picture under the stretched mapping. Commonly, it looks like some noises or irregular blocks.

Loss of details. The fine-level details in the target image are missed after the color transfer.

We note that it is not a special case. Ideally, color transfer between reference and target images should satisfy the following goals.

Color fidelity. The color distribution of the target should be close to that of the reference image.

Grain suppression. No visual artifacts (grain/blocky artifacts) should be generated in the target image.

Manuscript received May 22, 2013; revised October 21, 2013 and December 27, 2013; accepted January 09, 2014. Date of publication February 12, 2014; date of current version May 13, 2014. This work was supported in part by the National Natural Science Foundation of China (No. 61320106008), the NSFC-Guangdong Joint Fund (No. U1135003), the National Natural Science Foundation of China (No. 61103163, 61262050), and the Scholarship Award for Excellent Doctoral Student granted by the Ministry of Education 2012. The associate editor coordinating the review of this manuscript and approving it for publication was Prof. Adrian Munteanu.

Z. Su, L. Liu, and X. Luo are with the National Engineering Research Center of Digital Life, State-Province Joint Laboratory of Digital Home Interactive Applications, School of Information Science & Technology, Sun Yat-sen University, Shenzhen Digital Home Key Technology Engineering Laboratory, Research Institute of Sun Yat-sen University in Shenzhen, China.

K. Zeng is with the School of Software, Sun Yat-sen University, Guangzhou, China (e-mail: zengkun@gmail.com).

B. Li is with the School of Mathematics and Information Sciences, Nanchang Hangkong University, Nanchang, China.

Color versions of one or more of the figures in this paper are available online at http://ieeexplore.ieee.org.

Digital Object Identifier 10.1109/TMM.2014.2305914

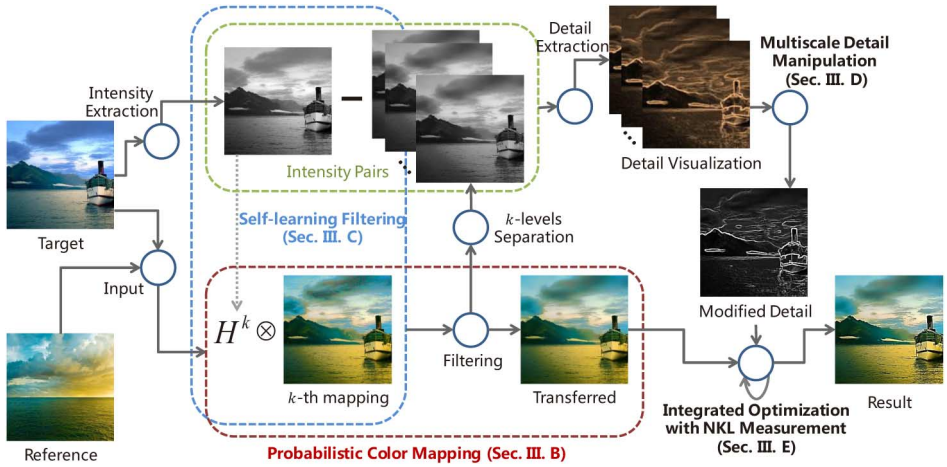

Fig. 2. The pipeline of our framework. In the procedure of the color transfer, the self-learning filtering scheme is integrated into the probability-based color distribution mapping to achieve triple functions, including color fidelity, grain suppression and detail manipulation. This integration has simple and efficient characteristics. We will demonstrate its effectiveness in the following sections and its applicability in lots of color-related applications.

Detail preservation. Details in the original target should be preserved after the transfer.

According to these goals, Xiao and Ma [4] pointed out that the color transfer problem can be formulated as the following optimization problem which minimizes the least squares error

$$\min\left(\sum\|\rho(r)-\rho(g)\|^2+\lambda\sum\|\nabla t-\nabla g\|^2\right), \quad (1)$$

where r, t and g denote the reference, target and transferred images. $\rho(\cdot)$ is the probability density function and ∇ is the gradient operator. However, there exists a major problem in the above equation. The Euclidean norm is not a suitable selection for measuring the color distribution. Eq. (1) is hard to directly solve, because the first term relates to probability distribution and the gradient operator in the second term is applied to the pixelwise image.

In this paper, we present a novel unified framework for example-based color transfer, which aims to achieve simultaneously grain suppression, color fidelity and detail preservation. The central to our approach is to incorporate a self-learning filtering scheme into the iterative probabilistic color mapping with minimizing normalized K-L distance as convergency. First, a probabilistic mapping is iteratively applied to generate coarse color mapping. Reducing the N-dimensional probability distribution of both reference and target to a one-dimensional probability distribution pair, it can match the color distribution of the target to the reference. Second, the self-learning filtering is embedded into the procedure of color mapping. By converting the original target into an uncorrelated space, the intensity channel is taken as the learning example into the filtering, which is further applied to the mapped result. The k-levels details can be extracted by the differential operator between the original target and the set of transferred outputs. Finally, the details are recombined to the transferred output to produce the result in a multilayer controllable manner. Our pipeline is sketched in Fig. 2.

We summarize our main contributions as follows.

- Propose a novel color transfer framework to achieve a unified corruptive artifacts suppression, which is specified in grain suppression, color fidelity and detail manipulation.
- Emphasize on the superiority of the self-learning filtering scheme in color transfer, rather than adopting post-processing remedies for the artifacts.
- Design a sort of objective and subjective measurements for the quality evaluation of color transfer to demonstrate the performance of our approach.
- Demonstrate our framework would be extended to some applications which is related with color editing.

II. Related Work

In this section, we just emphasize on the state-of-the-art automatic color transfer approaches but not those of interactive manipulations [8], and summarize their advantages and defects. In addition, the edge-preserving smoothing filters are introduced, so that we can discuss them for grain effect suppression and detail preservation in the following sections.

A. Color Transfer

The histogram matching (specification) [9] is able to specify the shape of the referred histogram that we expect the target image to have. However, histogram matching can only process the color components of the color image independently. Since the relationship of the color components are separated, this approach would produce the unsatisfactory look, e.g. grain effect, color distortion. Reinhard *et al.* [2] firstly proposed a way to match the means and variances between the target and the reference in the low correlated $L\alpha\beta$ color space. This approach was efficient enough, but the simple means and variances matching was likely to produce slight grain effect and serious color distortion. To prevent from the grain effect, Chang *et al.* [10], [11] proposed a color category-based approach that categorized each pixel as one of the basic categories. Then a convex hull was generated in $L\alpha\beta$ color space for each category of the pixel set, and the color transformation was applied with each pair of convex hull of the same category. For the color distortion, Tai *et al.* [12] proposed a modified EM algorithm to segment probabilistically the input images and construct Gaussian Mixture Models (GMMs) for them, and the relationship was constructed by each

Gaussian component pairs between the target and the reference under Reinhard's approach [2].

Abadpour *et al.* [13] proposed the exploited principal component analysis (PCA) and created a low correlated and independent color space to reduce the color correlation. Pitié *et al.* [3], [14] proposed an N-dimensional probability density function transfer approach to reduce the high-dimensional PDF matching problem to the one-dimensional PDF matching by Radon Transform [9]. This operation can reduce the color correlation and keep the color distribution of the transferred result consistent with that of the reference. However, it would lead to the variance of image contents as the pixel intensity changed. Therefore, the Poisson reconstruction was introduced to remedy the result. Inspired by the gradient domain technique, Xiao and Ma [4] proposed a gradient-preserving model to convert the transfer processing to an optimization, and balanced the color distribution and the detail performance. However, global optimal solution usually required large computational cost.

Dong *et al.* [15] proposed a dominant color idea for color transfer. When the amount of dominant colors of the target was consistent with that of the reference, the color of the reference would be transferred to obtain a satisfactory result. However, when the amount of dominant colors was not balanced, the unsatisfactory result would be produced. Wu *et al.* [16] improved Dong's approach [15] and further proposed a distribution-aware conception to consider the spatial color distribution in the reference image. And Wang *et al.* [17], [18] developed the learning-based color transfer methods to train out the proper color mapping relationship. Recently, HaCohen *et al.* [5] presented the non-rigid dense correspondence and used it in example-based color transfer. However, the corresponding requirements would limit the example selection. Pouli and Reinhard [6] proposed a progressive histogram reshaping technique for images of arbitrary dynamic range, which still suffers from color distortion in some extreme cases. In addition, Wong *et al.* [19] investigated the assessment of image realism for the evaluation of the image recoloring.

B. Edge-Preserving Smoothing

The grain effect can be treated as a special type of noises [14], and it would be removed by linear smoothing. Although the linear smoothing can remove the grains, the over-blurring would destroy the original image details and lower the sharpness of edges. Edge-preserving smoothing (EPS) filters [20]–[25] are proposed to overcome this problem. They can prevent the edge blurring by linear filtering according to their intensity- or gradient-aware properties. However, the performance of pure EPS filters is limited [26], [27], especially if there exists the corresponding version of the input image.

Joint bilateral filter (JBF) [28], [29] is the first guided edge-preserving smoothing approach. The JBF exploits the pixel intensity of the reference which is correlated to the target to improve the filtering effect. However, like the bilateral filter (BLF), JBF can not avoid the halo artifact and gradient reversal problem. Just like aforementioned Bae's approach [30], it requires the gradient correction to remedy the side-effect of BLF. He *et al.* [31] proposed the guided filter, which has the advantages of JBF but overcomes the defects.

In addition, based on the edge-preserving smoothing, the details can be extracted to manipulate in a multiscale way [32]. Fattal *et al.* [33] proposed an elaborate scheme for details, but their adoptive bilateral decomposition has defects as aforementioned. Farbman *et al.* [21] proposed two multiscale schemes which are simpler than Fattal's, because the WLS-based decomposition overcomes the defects of bilateral decomposition. And then, Farbman *et al.* [34] introduced the diffusion maps as a distance measurement to replace the Euclidean distance in their weighted least square filter. Recently, Paris *et al.* [35] explored the local Laplacian pyramid to yield the edge-preserving decomposition for fine-level detail manipulation.

III. Integrated Color Mapping Model

As mentioned in Section I, the example-based color transfer problem lies in seeking the reasonable mapping relationship between reference and target images, and a perfect color transfer approach should satisfy three goals at the same time, including the color fidelity, grain suppression and details preservation. Motivated by the probability-based mapping and edge-preserving decomposition, we present a novel unified transfer framework instead. The overview of our framework is as follows.

Color mapping stage. A probabilistic color mapping is applied to achieve the basic color corresponding and a self-learning filtering is embedded to avoid the artifacts and separate the transferred target into k levels.

Detail manipulation stage. A multiscale detail manipulation scheme is applied to preserve or enhance the details.

Integrated optimization stage. The transferred result and the modified details are combined into an optimization solution with the normalization Kullback-Leibler measurement to yield the final output.

A. Kullback-Leibler Distance for Color Transfer

The Kullback-Leibler distance (K-L) [36] can measure the similarity between two completely determined probability distributions. Here, we apply it to measure the difference between the reference r and transferred result g in color transfer. The minimization of K-L distance means the color appearance of the target close to that of the reference. Let $\rho(r)$ and $\rho(g)$ denote the distributions of the reference image and the transferred image, respectively, we have

$$\min D_{\mathrm{KL}}(\rho(g)\|\rho(r)) = \min \sum_j \rho_j(g) \ln \frac{\rho_j(g)}{\rho_j(r)}. \quad (2)$$

Taking the K-L distance as a measurement in an optimization procedure, to guarantee the convergence of minimization, we require Eq. (2) should satisfy the following constraint

$$D_{\mathrm{KL}}(\rho(g^{k+1})\|\rho(r)) \leq D_{\mathrm{KL}}(\rho(g^{k})\|\rho(r)), \quad (3)$$

where k is the iterative threshold in the solution. Essentially, $D_{KL}(\cdot)$ is a monotonically non-increasing and non-negative function, therefore it has a limit. $\lim D_{KL} = 0$, if the distribution $\rho(g)$ and $\rho(r)$ are equal. The above K-L distance is a fundamental measurement in our framework. We first break our solution into two phases. One is the color mapping; the other is

the detail manipulation. And then we give the integrated optimization framework in Section III-E.

B. Iterative Probabilistic Color Mapping

For given gray images, the probabilistic mapping relationship between the reference image and the transferred image is formulated as

$$\rho(g)dg = \rho(r)dr,\ \tau(g) = r. \tag{4}$$

Through establishing the discrete look-up tables, we can solve out the mapping relationship

$$\tau = C_r^{-1} C_g(g), \tag{5}$$

where C_r and C_g denote the cumulative distribution corresponding to $\rho(r)$ and $\rho(g)$, respectively. However, for color images, due to the correlated property of color channels, direct matching in Eq. (5) is likely to yield color distortion. In our framework, we exploit a decorrelation to tackle this issue. This decorrelation would be regarded as a piece-wise homography transformation with an iterative process. It is parameterized as the projection with the randomized orthogonal transform in the following

$$\mathcal{H} = [I|\mathcal{R}]^{\mathbf{T}} \times Q_n, \tag{6}$$

where I is a 3×3 identity matrix and $\mathcal{R}$ is a 3×3 homography coefficient matrix as a rotation projection. Q_n is a randomized orthogonal matrix used for n times iteration. In our implementation, we initial $\mathcal{R} = [2/32/3 - 1/3; 2/3 - 1/32/3; -1/32/32/3]$. This setting can make the rotation satisfy the orthogonality. Afterward, a channel quantization with step Δq is used to control the scale of data range, which is parameterized by the pixel intensity or user setting. This quantization can guarantee the scale consistence in different date range of the rotated channels. Then, the corresponding 1-D probability density distributions of both target and reference are yielded by the probability statistics similar to the image histogram.

By the decorrelation, we use the following iterative scheme to solve out the transferred result

$$g^{k+1} = g^k + \mathcal{H}^{\mathbf{T}} \left[\tau\left(\mathcal{H}g^k\right) - \mathcal{H}g^k\right]. \tag{7}$$

The physical meaning of Eq. (7) could be interpreted as follows. The projection of 1-D probability density is obtained by homography transformation $\mathcal{H}$, and the k-th mapping result is calculated. Then, the difference between before and after mapping is evaluated by $[\tau(\mathcal{H}g^k) - \mathcal{H}g^k]$. The inverse transformation is used to restore the 2D image. Finally, the intermediate g^k is updated and a cycle of iteration is completed. The illustration of the iterative probabilistic color mapping is shown in Fig. 3.

C. Self-learning Filtering Scheme

However, there still exists a defect in the solution in Section III-B, that is, it is likely to produce the grain effects occasionally. To address this challenging problem, we present a self-learning filtering scheme and incorporate it into the aforementioned iterative probabilistic color mapping. Firstly,

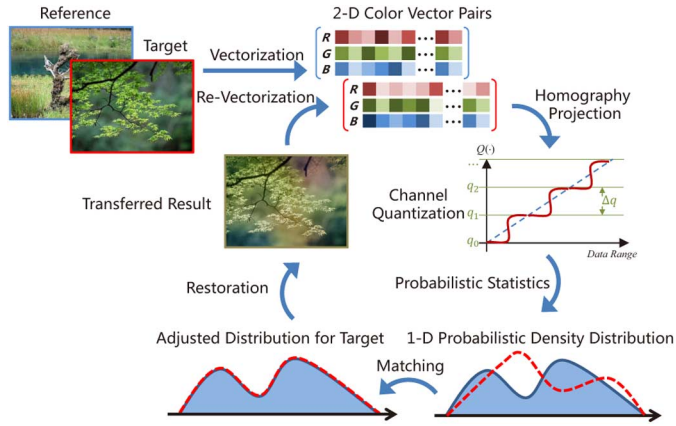

Fig. 3. The probability-based color distribution mapping with minimizing K-L distance. In an iterative cycle, the reference image and the target image are transformed into 2-D color vector pairs. By the homography projection and probabilistic statistics with channel quantization, we obtain the 1-D distribution on directive axes. The probability distribution of the target matches to that of the reference. The restoration is performed to output the transferred result. The iteration would be stopped until reach the preset times or minimized error.

assume the transferred result g and its filtered output $\hat{g}$ are divided into a series of 9×9 patches, and each patch-pair has 1-to-1 corresponding relationship. Then, we further assume that g and $\hat{g}$ have the following linear learning relationship in the patch p_κ

$$\hat{g}_i = \alpha_\kappa g_i + \beta_\kappa, \forall i \in p_\kappa, \tag{8}$$

where α_κ and β_κ are linear coefficients. Subscripts i and κ are used for pixels and patches indexing, respectively. Let μ_κ and σ_κ^2 be the mean and variance of g in p_κ, $|p|$ is the pixel amount of p_κ. Using the least squares parameter estimation, α_κ and β_κ can be estimated by

$$\alpha_\kappa = \frac{\frac{1}{|p|}\sum_{i \in p_\kappa} g_i \hat{g}_i - \mu_\kappa \overline{\hat{g}_\kappa}}{\sigma_\kappa^2},\ \beta_\kappa = \overline{\hat{g}_\kappa} - \alpha_\kappa \mu_\kappa, \tag{9}$$

where $\overline{\hat{g}_\kappa} = \frac{1}{|p|}\sum_{i \in p_\kappa} \hat{g}_i$. However, $\hat{g}$ is an unknown variable. To determine α_κ and β_κ, we replace $\hat{g}$ by the target image t. Then, Eq. (9) is reformulated as

$$\alpha_\kappa = \frac{\frac{1}{|p|}\sum_{i \in p_\kappa} g_i t_i - \mu_\kappa \overline{t_\kappa}}{\sigma_\kappa^2 + \varepsilon},\ \beta_\kappa = \overline{t_\kappa} - \alpha_\kappa \mu_\kappa, \tag{10}$$

where ε is used to compensate the error caused by the substitution. Since each patch-pair has α_κ and β_κ, the overlaps can be treated by averaging $(\bar{\alpha}_\kappa, \bar{\beta}_\kappa) = \frac{1}{|p|}\sum_\kappa (\alpha_\kappa, \beta_\kappa)$. In essence, the self-learning filtering is an edge-preserving smoothing operation under linear regression with reference image. We presented our result with this scheme and compared it with Pitiè's in Fig. 4 and Fig. 5.

D. Multiscale Detail Manipulation Scheme

As mentioned in Section I, details in the original target should be preserved after the transfer. Actually, details often correlate to the style appearance, and this characteristic is significant to the color-related applications. Since we have incorporated the self-learning filtering scheme into the color mapping, we can exploit its property of edge-preserving decomposition to extract

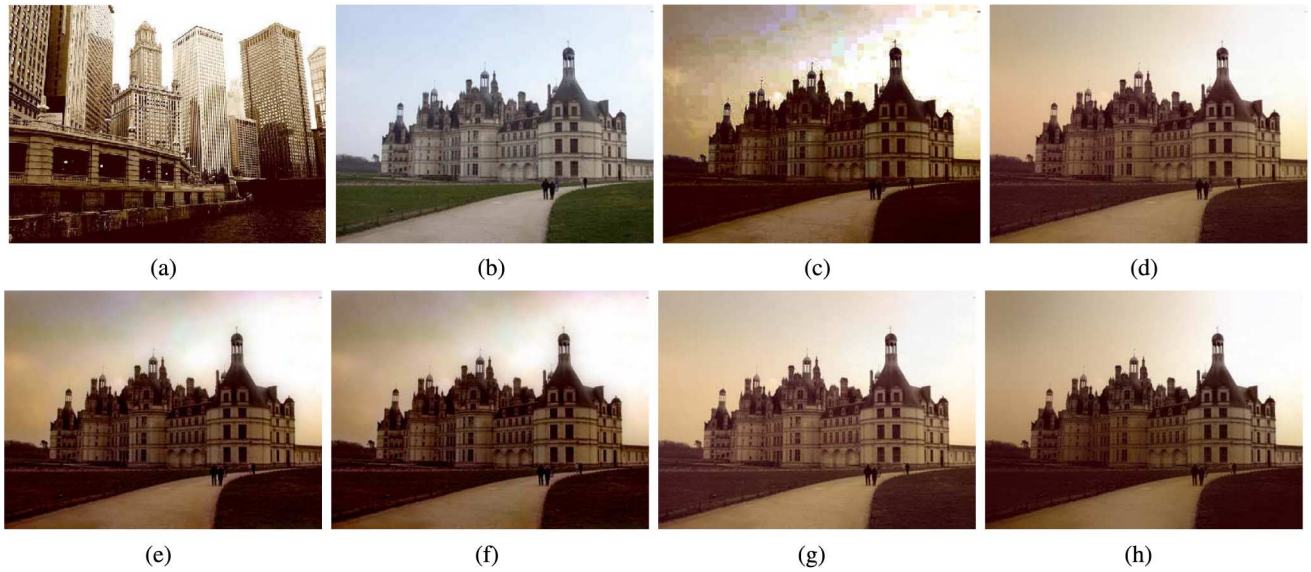

Fig. 4. The comparison of the integrated color mapping model and Pitié's approach [14]. (a) Reference. (b) Target. (c) Pitié's N-dimensional PDF step ($n = 10$). There are obvious grain effect and content distortion in (c), e.g. the tone of the clouds. (d) Our improved result ($k = 8, \varepsilon = 1e-3$). We obtained a visual satisfactory result under the self-learning filtering scheme. Furthermore, we compared the N-dimensional PDF added Poisson editing [14] in (e)-(f) with our approach in (g)-(h). (e) $n = 3, \lambda = 1$. (f) $n = 10, \lambda = 1$. (g) $k = 3, \varepsilon = 1e-3$. (h) $k = 10, \varepsilon = 1e-3$.

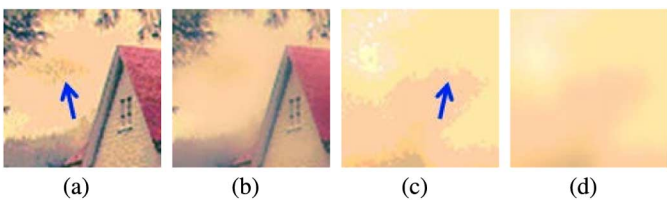

Fig. 5. Self-learning filtering scheme for grain suppression. Note the grain effect can be smoothed while the edge can be preserved.

the details while compensating or enhancing them in the transferred output. In our framework, k-levels details d^k are obtained by iteratively applying the self-learning filtering scheme. The sigmoid function is further brought to avoid the hard clipping that would occur when the detail levels are significantly boosted. To sum up, the multiscale detail manipulation scheme is formulated as

$$M(d^k, \lambda) = \begin{cases} \frac{1}{k}\sum_{i}^{k} d^k, & \lambda = 1, \\ \sum_{i}^{k} \frac{1}{(1+e^{-\lambda d^k})}, & \lambda \neq 1, \end{cases} \tag{11}$$

where λ is the adjustment factor for preserving ($\lambda = 1$) or enhancing ($\lambda \neq 1$) the details. The comparison of detail enhancement is shown in Fig. 6.

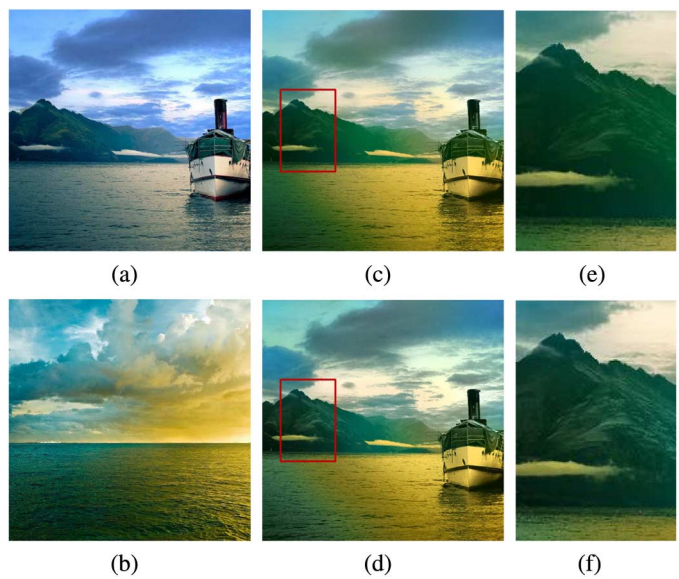

Fig. 6. Detail enhancement. (a) Target. (b) Reference. (c) Without enhancing ($\lambda = 1$). (d) Detail enhancing ($\lambda = 3$). The specified magnified regions corresponding to (c) and (d) are shown in (e) and (f), respectively. Obviously, more details are presented in (f) than in (e).

E. Integrated Optimization Framework

In Section III-A, we presented the K-L distance can be used to evaluate the similarity between the color distribution of the reference image and that of the transferred image. For more robust, we prefer to use the normalized form instead

$$D_{\mathrm{NKL}} = \left(D_{\mathrm{KL}} - D_{\mathrm{KL}}^{\min}\right) / \left(D_{\mathrm{KL}}^{\max} - D_{\mathrm{KL}}^{\min}\right). \tag{12}$$

Then, according to Section III-A–III-D, we summarize our color transfer framework with minimizing the normalized K-L distance in the following

$$\min D_{\mathrm{NKL}}\left(\rho\left(S(\hat{g}, t) + M(d, \lambda)\right) \| \rho(r)\right), \tag{13}$$

where $S(\cdot)$ and $M(\cdot)$ denote the self-learning filtering operator and detail manipulation operator, respectively. With this unified framework, we achieve our aforementioned goals seamlessly, including grain suppression, color fidelity and detail preservation. The pseudo code of our approach is given in Algorithm 1. Our results are presented in Fig. 4 and Fig. 7.

Fig. 7. The influence of parameter settings. (a) Reference. (f) Target. (b) The grain effect. From (c) to (e) are the effects of grain suppression by self-learning filtering. (c) $\varepsilon = 1e-2$. (d) $\varepsilon = 1e-3$. (e) $\varepsilon = 1e-4$. From (g) to (j), fixing $\varepsilon = 1e-3$, the results are obtained by adjusting the iteration times k and the detail enhancement factor λ. (g) $k = 1, \lambda = 1$. (h) $k = 3, \lambda = 1$. (i) $k = 5, \lambda = 2$. (j) $k = 10, \lambda = 2$.

Algorithm 1: Integrated Color Mapping Model

Input: t: target image, r: reference image, k: iterative times, ε: regularization factor, λ: detail factor

Output: g: transferred result

$g^0 = t, i = 0, \delta = D_{\mathrm{NKL}}(t, r)$ % Initialization
while $i < k$ **do**
  while $\delta^i = D_{\mathrm{NKL}}(g, r) \geq \delta^{\max}$ **do**
    $\mathcal{H} = [I, \mathcal{R}] * orth(rand(Q_n))$ % Homography Transformation
    $G = \mathcal{H}^{\mathbf{T}} g^i,\ R = \mathcal{H}^{\mathbf{T}} r$
    $S_{\min} = \min(G, R),\ S_{\max} = \max(G, R)$
    $S = (S_{\max} - S_{\min})/q$ % q steps of quantization for $G\&R$
    $\rho(g^i) = \mathrm{Hist}(S, G),\ \rho(r) = \mathrm{Hist}(S, R)$
    $\tau = \mathrm{HistMatch}(\rho(g^i), \rho(r))$ % 1D distribution matching
    $g^{i+1} = g^i + \mathcal{H}[\tau(G) - G]$ % Iterative update
    $\alpha = (\frac{1}{|p|} \sum t(g^{i+1}) - \mu\overline{g^{i+1}})/(\sigma^2 + \varepsilon)$
    $\beta = \overline{g^{i+1}} - \alpha\mu$
    $\hat{g} = \alpha * g^{i+1} + \beta$ % Apply self-learning filtering
    $d = t - \hat{g}$
    $g^{i+1} = \hat{g} + M(d, \lambda)$ % Detail manipulation
  end while δ
end while k
return

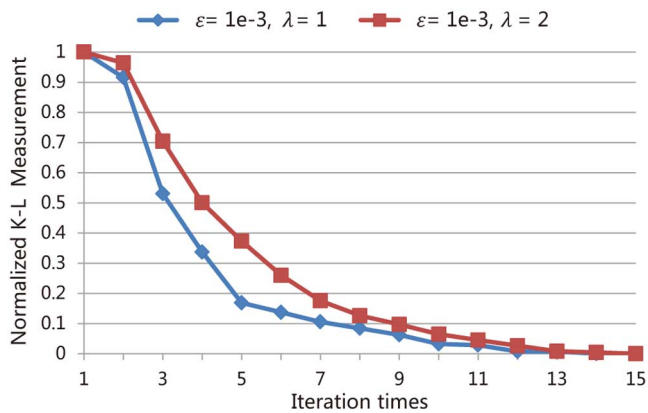

Fig. 8. Convergence analysis. The test samples are corresponding to Fig. 7(a) and (f). The blue line is the normal transfer without detail enhancement. And the red line is corresponding to the enhancement $\lambda = 2$. With the iteration increasing, the values of K-L distance are reducing. That means the color distribution of the transferred result gets close to that of the reference progressively. Some results are shown in Fig. 7(g)–(j).

IV. Experimental Analysis

In this section, we firstly discuss the parameter settings and the convergence in our framework. Then, we compare our framework with the state-of-the-art approaches in the visual effects and distribution visualization. To further demonstrate the effectiveness, we design a user investigation to aid the analysis. At last, the runtime performance is presented. All the experiments were tested on PC with Intel i5-2450M 2.5 GHz CPU, NVIDIA 610M, 4 GB DDR3 Ram, and MATLAB R2012a.

A. Parameter Setting and Convergence Analysis

Our framework refers to 4 adjusted parameters, including the radius r of patch p_κ in self-learning filtering, the regularization factor ε to compensate the error caused by the substitution, the iteration k and the detail enhancement factor λ. We will analysis the performance by adjusting these parameters. The proposed self-learning filtering scheme is used to prevent the error accumulation of grain effect or color distortion with the iteration increasing in color transfer. The effect of self-learning filtering

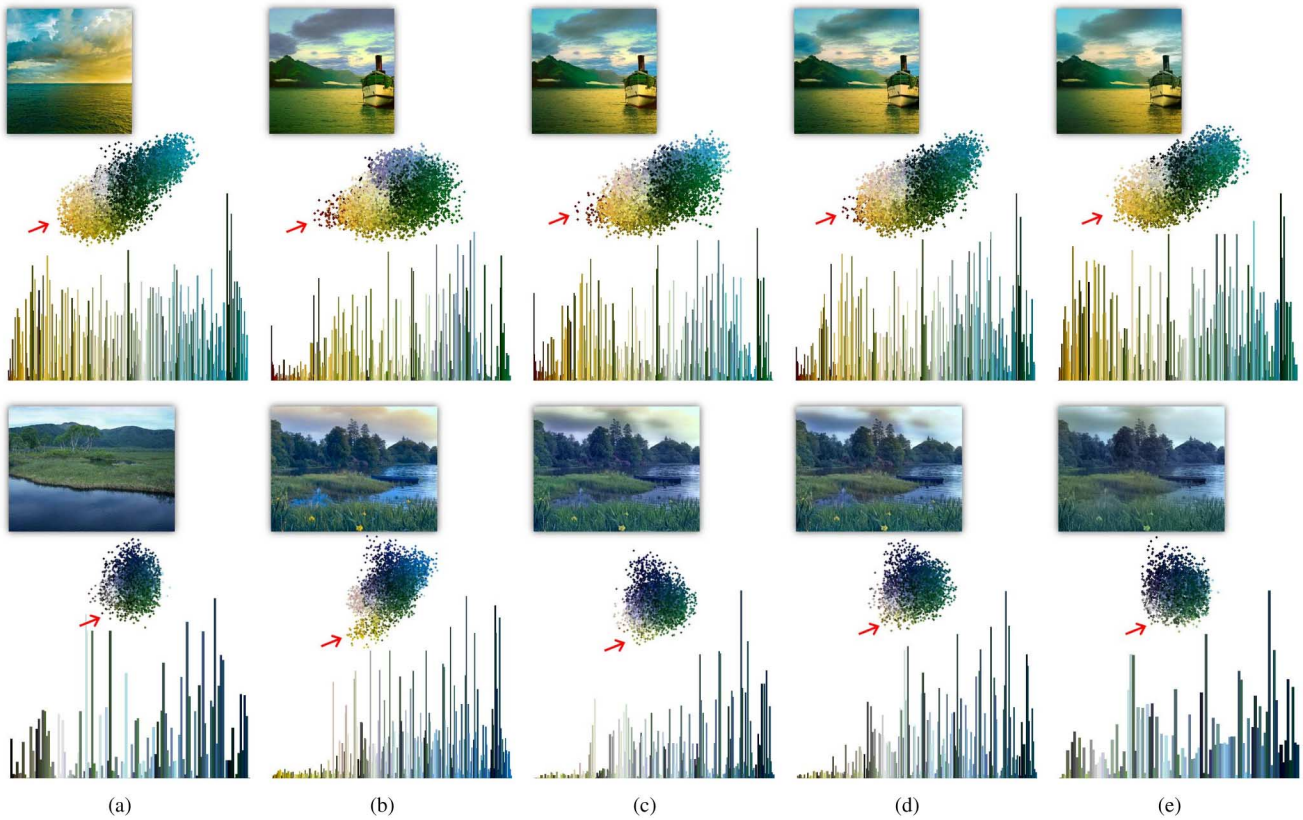

Fig. 9. The comparisons of color distribution with the state-of-the-art approaches and ours. (a) References. (b) Reinhard's results [2]. (c) Gradient-preserving results ($\lambda = 1$) [4]. (d) Pitié's results ($n = 10$, $\psi = 1$) [14]. (e) Our results ($k = 4$, $\varepsilon = 1e - 3$). All the parameter settings are corresponding to the reference work, respectively. From the 1-D and 2-D distributions, we can discriminate the color distortion intuitively. Our results have more similar distribution shapes than those of comparative approaches.

is determined by the radius r of patch p_κ and the regularization factor ε. The former restricts the action scope and affects the strength of the smoothing; the latter is used to balance the edge/detail preservation and the image smoothing. To be simplified, we fixed the radius $r = 20$ in all of our experiments empirically. And the effect of grain suppression depends on the setting of ε. The grain effect is shown in Fig. 7(b). In Fig. 7(c)–(e), we selected three magnitudes in which $\varepsilon = [1e-2, 1e-3, 1e-4]$. Observing the results in Fig. 7(c)–(e), we can see the grain effect has been suppressed and the details have been persevered progressively.

Our framework exploits the normalized Kullback-Leibler distance to measure the similarity of color distribution between the transferred output and the reference image, and ensures the convergence during the iterative procedure. We present the convergence curves in Fig. 8. The tested inputs were corresponding to the reference and the target in Fig. 7. The blue curve presents the convergent case without the detail manipulation ($\lambda = 1$), and the red curve presents the case with 2 times enhancement ($\lambda = 2$). See from Fig. 8, with the iteration increasing, the measured K-L values become lower. This means the color distribution of the transferred result is more and more close to that of the reference. For the above two cases, we give 4 groups of parameter settings ($k = 1$, $\lambda = 1$), ($k = 3$, $\lambda = 1$) ($k = 5$, $\lambda = 2$), ($k = 10$, $\lambda = 2$) in Fig. 7(g)–(j). Compared with these results in visual, the color appearance of the results get closer to the reference progressively with the iteration increasing.

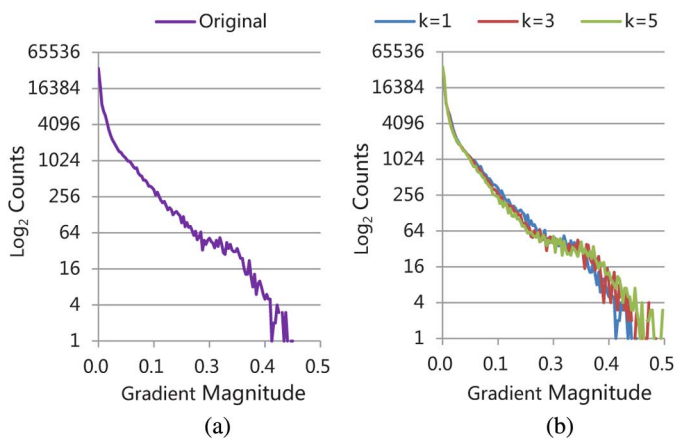

Fig. 10. Statistical gradient distribution. (a) Original target. (b) Our results. We counted the gradient magnitudes and plotted them as distribution curve in Log_2 pattern. Compared the gradient magnitude of the original target with those of the transfer results, we found that our results were very close to the original target in the gradient distributions.

B. Color Distribution Comparisons and Measurement

Although we can evaluate the results by visual observing directly, the geometric distribution of the colors in the image would not always be presented as the region assemble but possible dispersion. At this time, it is hard to evaluate the quality of the transferred results by visual observing merely. In our opinion, converting the image to 1-D color histogram and 2-D

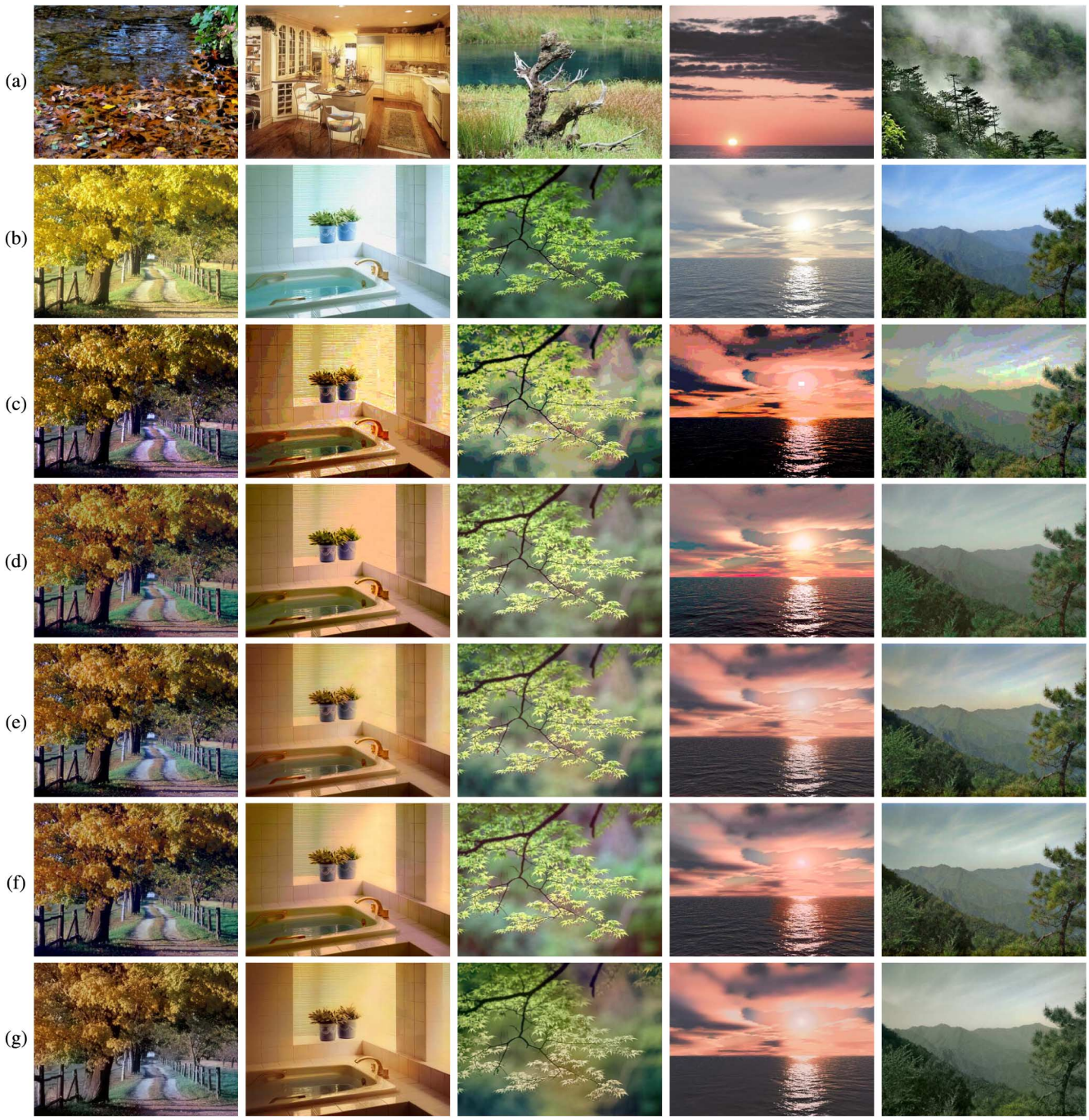

Fig. 11. The visual comparisons. (a) Reference. (b) Target. (c) Histogram matching [9]. (d) Reinhard's results [2]. (e) Pitié's results ($n = [10, 10, 3, 3, 10]$, $\psi = 1$). (f) Gradient-preserving results (all in $\lambda = 1$) [4]. (g) Our results ($k = [1, 3, 3, 3, 4]$, $\varepsilon = 1e - 3$). We recommend the electronic version for a high resolution.

color scatter diagram, we can observe the shapes of color distribution to evaluate the quality intuitively. In Fig. 9, we presented two groups of analyzed results. From the top row results in Fig. 9(b)–(d), some new colors appear in the transferred result (red dots and bars), which are not contained in the reference. By contrast, our result is faithful to the color appearance of the reference. In the bottom row, note the most left side in 1-D color histogram, the results in Fig. 9(b)–(d) have obvious color distortion. However, our result has the most similarity to the color distribution of the reference. Through these visualization approaches, we can further measure the quality of transferred results objectively.

Xiao *et al.* [4] emphasized the gradient-preserving was a significant characteristic that should not be ignored. Here, we designed a statistical gradient distribution to evaluate our approach. The gradient distribution of the original target is shown in Fig. 10(a). Our results with different parameter settings are shown in Fig. 10(b). Through these comparisons, we can demonstrate the gradient distributions of our results are similar to that of the original target.

TABLE I
THE K-L MEASUREMENT OF A PORTION OF TESTED IMAGES. ALL THE RECORDS ARE EVALUATED IN MATLAB 2012A

No.	Hist	Reinhard	GradPrev	NPDF	Ours
Fig. 9(top)	23.42	0.1259	0.0991	0.0284	0.0253
Fig. 9(bottom)	23.31	0.3639	0.1547	0.1037	0.0493
Fig. 11. c1(left)	21.47	0.3238	0.1302	0.0810	0.2112
Fig. 11. c2	22.79	0.2781	0.2173	0.0716	0.0949
Fig. 11. c3	23.02	0.4225	0.1861	0.2435	0.0354
Fig. 11. c4	25.28	0.6976	0.4112	0.2524	0.133
Fig. 11. c5(right)	22.85	1.2167	0.1347	0.1440	0.1116

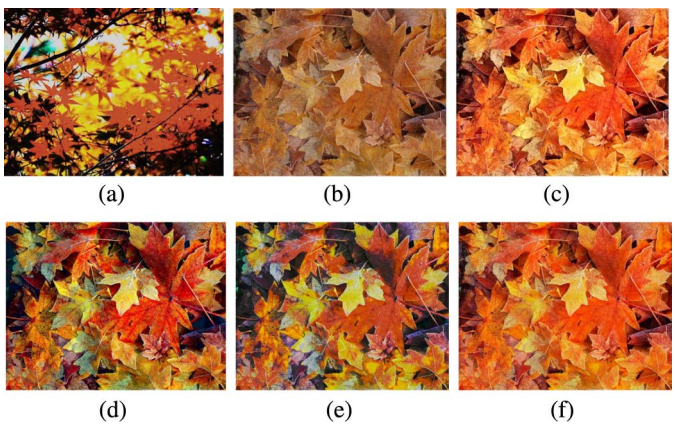

Fig. 12. Comparison with Wang's experiments [18]. (a) Reference. (b) Target. (c) Wang's result. (d) Pitié's result [37]. (e) Our result which refers to (a). (f) Our result which uses the same color components as Wang's with $k = 3, \varepsilon = 1e{-}4$.

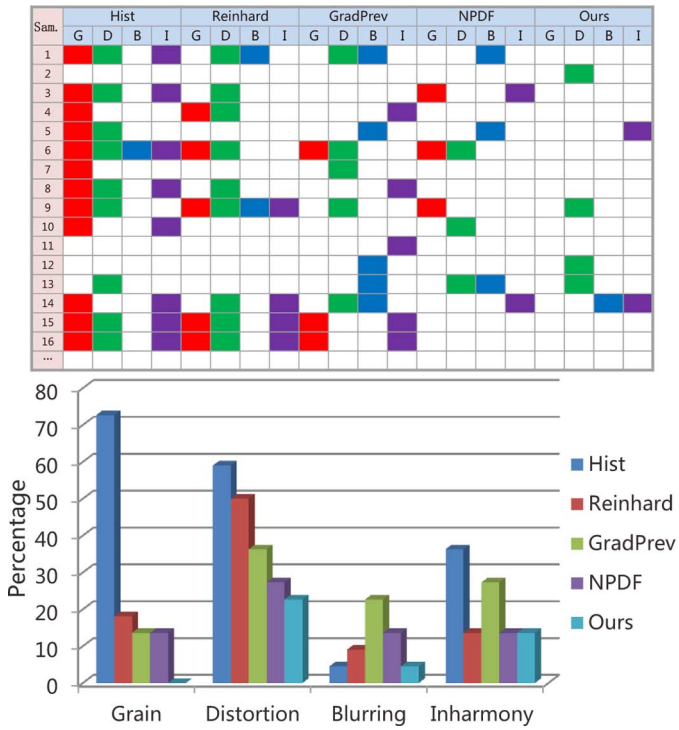

Fig. 13. User investigation. 100 samples are listed and 10 persons participated in the investigation. The top figure is a record in our experiments. Grain effect (G), color distortion (D), blurring (B) and inharmony (I) are evaluated by users' visual perception. The bottom figure is a statistical analysis for our investigation. The lower percentage means the better visual performance.

Our normalized K-L measurement would be extended to evaluate the quality of the transferred results which are produced by different approaches. We measured the results in Fig. 9 and Fig. 11, and recorded their K-L values in Table I. Note the data, histogram matching [9] has a terrible performance, and the K-L values are far above the values of other approaches. From the visual observation, the results of histogram matching are not acceptable. The Reinhard's approach [2] is likely to produce the color distortion, so its K-L values are high in some cases. The Pitié's N-dimensional PDF [14] and Xiao's GradPrev [4] have acceptable K-L values. For our results, the recorded performances are better than those of previous approaches.

In Fig. 12, we compare with Wang's experimental results [18]. Actually, if we consider the color consistence between the reference image and the transferred result, we found that it is not easy to say Wang's result is better than Pitié's and ours, see Fig. 12(c)–(e). By contrast, if we limit the color components as Wang's, our approach would produce a style appearance similar to Wang's result, see Fig. 12(f).

C. User Investigation

To further demonstrate the effectiveness of our framework, we design a user investigation with subjective experiments. We summarized 4 types of major defects in color transfer, including grain effect, color distortion, blurring, and distribution inharmony. In the statistical sense, we provided 100 groups of experimental data, and recorded the results which were produced by histogram matching [9], Reinhard's [2], Pitié's N-dimensional PDF with Poisson editing [14], Xiao's gradient-preserving approach [4] and ours. We invited five males and five females to participate, including 2 professional designers, 5 masters and 3 teachers. As illustrated in Fig. 13(top), the opinions of each person are recorded and presented in visualization. With all the investigated results, we can evaluate the statistical results. See from Fig. 13(bottom), histogram matching has serious grain effect and color distortion in actual cases. Reinhard's approach has a higher percentage in color distortion as well. And the Xiao's and Pitié's approaches are likely to produce the blurring. By contrast, our framework has a better performance than the previous approaches in the aforementioned 4 aspects. The investigation results are consistent with the above objective and subjective results.

D. Time Performance

We adopted the experimental runtime to measure our approach, and compared it with other approaches. We selected 5 sizes as the tested samples ($256^2 - 2048^2$). The runtimes with various parameter settings were recorded in Table II. See from the Table II, histogram matching [9] and Reinhard's approach [2] had an efficient runtime response. However, as mentioned above, both of them were hard to obtain a satisfactory visual performance. Xiao's gradient-preserving approach [4] and Pitié's N-dimensional PDF approach [14] required too much time, because both of them needed to solve a large-scale optimization equation. Especially, if the size was over large, these two approaches would break down. By contrast, our approach had a

TABLE II
THE RUNTIME COMPARISONS OF THE TESTED TRANSFER APPROACHES. ALL THE RECORDS ARE EVALUATED IN MATLAB 2012A (UNIT: SECOND)

	Par.	$(256)^2$	$(512)^2$	$(1024)^2$	$(1600)^2$	$(2048)^2$
Hist	–	0.169	0.256	0.417	0.771	1.055
Rein.	–	0.028	0.112	0.422	0.877	1.620
Grad.	λ=1	2.572	8.921	36.08	–	–
NPDF	n=1	2.302	8.546	33.73	–	–
	n=3	2.624	9.656	38.21	–	–
	n=10	3.727	13.57	53.41	–	–
Ours	n=1	0.380	1.354	4.833	11.90	19.26
	n=3	0.838	3.481	13.66	34.25	56.31
	n=10	2.545	11.04	44.75	115.1	189.7

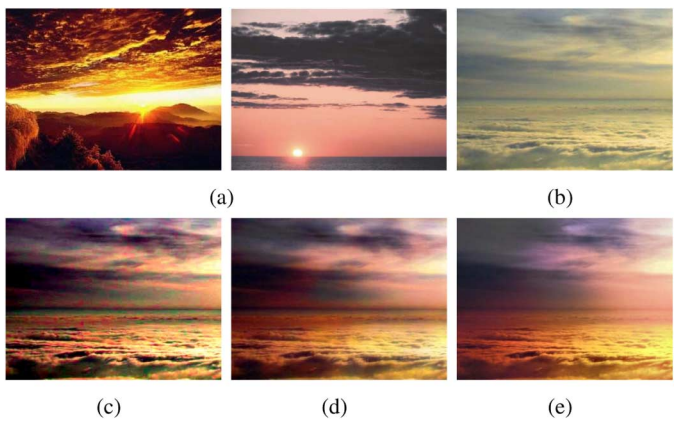

Fig. 14. Multiple-reference color transfer. (a) References with the sunshine topic. (b) Target. (c) A serious grain effect appears in Reinhard's result. (d) A slight grain effect appears in Pitié's result ($n = 10$) as well. (e) Our result ($k = 8, \varepsilon = 1e-3$). The colors of multiple references are blended evenly to produce a visual satisfactory output.

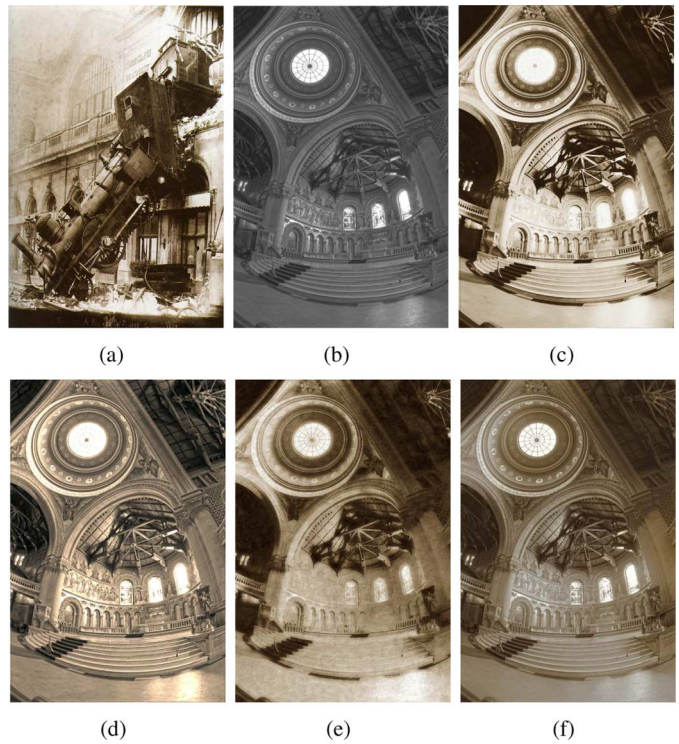

Fig. 15. Our framework can seamlessly handle HDR images. (a) Ancient photo. (b) LDR output was produced by Photoshop CS5. (c) Histogram matching. (d) Reinhard's. (e) Bae's Two-scale approach. (e) Ours ($k = 3$, $\varepsilon = 1e-3$). Note the windows on the church roof and the whole tone appearance.

sound time response and was better than previous approaches in usability.

V. VISUAL APPLICATIONS

In this section, we extend our framework to some image applications, including multiple-reference color transfer, high-dynamic-range color transfer and style transfer. Through these extended applications, we further demonstrate the applicability of our framework.

Multiple-reference color transfer requires the transfer naturally blending the colors from multiple references. However, as illustrated in Fig. 14(a), the main difference exist among the references. Although both of the references are the sunshine theme, they have a big difference in the color appearance. This difference would easily lead to the grain effect in the result. As illustrated in Fig. 14(c), the Reinhard's result has a serious grain effect. Pitié's approach adopts the gradient correction to suppress the grain, but it does not prevent the color distortion, see Fig. 14(d). Our approach deals with the grain effect and distortion in each step, therefore, we can achieve a visual satisfactory result, see Fig. 14(e).

High-dynamic-range (HDR) color transfer requires considering the image contents fidelity and the color appearance. The low-dynamic-range image is produced by the HDR tools in Photoshop CS5 and shown in Fig. 15(b). The results of histogram matching and Reinhard's are shown in Fig. 15(c)–(d), respectively. Note the results, histogram matching cannot display the whole contents effectively; and the Reinhard's approach exhibits obvious color distortion. Bae *et al.* [30] exploit their approach to create a "soft-yet-sharp" rendition which is a convincing approximation of the effect produced by a soft-focus lens. Their effort would produce a slight blurring, see Fig. 15(e). However, blurring is not always expected in color transfer. By our approach, we can obtain a clear output, in which the contents and the details are displayed with a sound visual performance.

Style transfer is a basic requirement in art design. Lots of image styles can be reflected by the color appearance, e.g. the ancient, cold and rainbow styles in Fig. 16(b). We demonstrated our approach can effectively preserve the style of the reference in Fig. 16(c).

VI. DISCUSSIONS AND CONCLUSIONS

How to transfer the colors of the given reference to the target effectively is a challenging problem and is significant in color transfer. Because of the complexity of the color distribution, it is difficult to avoid the corruptive artifacts such as color distortion, grain effect or loss of details in the result of color transfer. When these problems appear, the traditional way is to apply some post-processing operations to remedy them, e.g. Bae's [30], Pitié's [14] and Xiao's [4]. Unfortunately, the post-processing operations are not always effective and would cause other artifacts sometimes.

(a) (b) (c)

Fig. 16. Style Transfer. (a) Target. (b) A group of references, including ancient, cold, and rainbow styles. (c) Results. The artistic styles are produced by Photoshop CS5. In this experiment, we set the parameters $k = 5, \varepsilon = 1e-3$.

TABLE III
GLOSSARY OF MAIN TERMS

Symbol	Description
r	the reference image
t	the target image
g	the transferred goal image
k	iteration times
τ	the mapping relationship
$\mathcal{H}$	the decorrelation operator for color image
Δq	the step for channel quantization
$\hat{g}$	the output of self-learning filtering
$\alpha_\kappa, \beta_\kappa$	the linear coefficients of filtering in the patch p_κ
$\mu_\kappa, \sigma_\kappa^2$	the mean and variance of g in p_κ
ε	smooth factor for filtering
d^k	k-levels details
λ	the adjustment factor for detail manipulation
$\rho(\cdot)$	probability distribution function for images
$C(\cdot)$	cumulative distribution function for images
$S(\cdot)$	the self-learning filtering operator
$M(\cdot)$	the detail manipulation operator
$D_{\mathrm{NKL}}(\cdot)$	normalized K-L measurement function

In this paper, we proposed a novel color transfer framework to deal with these corruptive artifacts by integrated a self-learning filtering scheme into the iterative probabilistic color mapping model. Our framework not only prevents the color distortion and grain effect in the process of transfer, but also achieves the effect of detail preserving or enhancing. In addition, to evaluate the quality of color transfer, we proposed a series of objective and subjective measurements, including convergence analysis, shape analysis of color distribution, visual comparison and user investigation. By the experimental analyses in the objective and subjective data, we found that our framework had a better performance than the state-of-the-art approaches, especially in dealing with the grain effect, color distortion, and loss of details. In addition to the one-to-one transfer, our framework was extended to the multiple-reference color transfer, HDR color transfer and style transfer to demonstrate its flexibility. For convenient, we summarized our symbols and notations in Table III.

(a) (b) (c)

Fig. 17. Limitations. (a) Theme colors. (b) Target. (c) Result ($k = 5, \varepsilon = 1e-3$). If the colors in the reference are excessively limited, our approach is likely to produce the bleeding-like effect in the result.

Strength and limitations. Our framework can achieve the color fidelity, prevent the grain effect and preserve the detail seamlessly. Without solving the large-scale optimization equation, our framework has a sound runtime response, see Table II. Our framework presents the convenience in dealing with the complicated colors, owing to that it only requires to provide the expected references but no other auxiliary interactions.

However, our framework still has some limitations. If the amount of the referred colors is limited, it is likely to produce two major problems. One is the inharmony of color appearance; the other is the color bleeding-like artifacts. As illustrated in Fig. 17, the specified reference is given in Fig. 17(a), and the obvious color inharmony appears in the whole image and the bleeding-like effect appears on the hill in Fig. 17(c).

In the future, we will extend our framework to video editing. A difficulty in video color transfer is the color consistent problems in the continuous frames, due to that the pixel colors would have a slight offset if the contents change in the video sequences. And how to be aware of the locations of the colors is also a critical problem. In addition, to overcome the above limitations in our approach to enhance the style appearance needs our continuous efforts.

ACKNOWLEDGMENT

We would like to thank Prof. Jiaya Jia and Dr. Li Xu for inspiring discussions and encouragement, the associate editor Prof. Adrian Munteanu and anonymous reviewers for their constructive comments.

REFERENCES

[1] T. Welsh, M. Ashikhmin, and K. Mueller, "Transferring color to greyscale images," *ACM Trans. Graph.*, vol. 21, no. 3, pp. 277–280, 2002.
[2] E. Reinhard, M. Ashikhmin, B. Gooch, and P. Shirley, "Color transfer between images," *IEEE Comput. Graph. Applicat.*, vol. 21, no. 5, pp. 34–41, 2001.
[3] F. Pitié, A. C. Kokaram, and R. Dahyot, "N-dimensional probablility density function transfer and its application to colour transfer," in *Proc. 10th IEEE Int. Conf. Computer Vision*, 2005, vol. 2, pp. 1434–1439.
[4] X. Xiao and L. Ma, "Gradient-preserving color transfer," *Comput. Graph. Forum*, vol. 28, no. 7, pp. 1879–1886, 2009.
[5] Y. HaCohen, E. Shechtman, D. B. Goldman, and D. Lischinski, "Non-rigid dense correspondence with applications for image enhancement," *ACM Trans. Graph.*, vol. 30, no. 4, pp. 70:1–70:10, 2011.
[6] T. Pouli and E. Reinhard, "Progressive color transfer for images of arbitrary dynamic range," *Comput. Graph.*, vol. 35, no. 1, pp. 67–80, 2011.
[7] T. Pouli and E. Reinhard, "Example-based color image manipulation and enhancement," in *Proc. ACM SIGGRAPH 2012Courses, ser. SIGGRAPH '12*, 2012, pp. 3:1–3:62.

[8] C. Xiao, Y. Nie, and F. Tang, "Efficient edit propagation using hierarchical data structure," *IEEE Trans. Visualiz. Comput. Graph.*, vol. 17, no. 8, pp. 1135–1147, 2011.
[9] R. C. Gonzalez and R. E. Woods, *Digital Image Processing*, 3rd ed. Upper Saddle River, NJ, USA: Prentice Hall, 2008.
[10] Y. Chang, S. Saito, and M. Nakajima, "Example-based color transformation of image and video using basic color categories," *IEEE Trans. Image Process.*, vol. 16, no. 2, pp. 329–336, 2007.
[11] Y. Chang, S. Saito, K. Uchikawa, and M. Nakajima, "Example-based color stylization of images," *ACM Trans. Appl. Percept.*, vol. 2, no. 3, pp. 322–345, 2005.
[12] Y. Tai, J. Jia, and C. Tang, "Soft color segmentation and its applications," *IEEE Trans. Pattern Anal. Mach. Intell.*, vol. 29, no. 9, pp. 1520–1537, 2007.
[13] A. Abadpour and S. Kasaei, "An efficient PCA-based color transfer method," *J. Visual Commun. Image Represent.*, vol. 18, no. 1, pp. 15–34, 2007.
[14] F. Pitié, A. Kokaram, and R. Dahyot, "Automated colour grading using colour distribution transfer," *Comput. Vision Image Understand.*, vol. 107, no. 1-2, pp. 123–137, 2007.
[15] W. Dong, G. Bao, X. Zhang, and J.-C. Paul, "Fast local color transfer via dominant colors mapping," *ACM SIGGRAPH Asia 2010Sketches*, pp. 46:1–46:2, 2010.
[16] F. Wu, W. Dong, X. Mei, X. Zhang, X. Jia, and J.-C. Paul, "Distribution-aware image color transfer," *ACM SIGGRAPH Asia 2011Sketches*, pp. 8:1–8:2, 2011.
[17] B. Wang, Y. Yu, T.-T. Wong, C. Chen, and Y.-Q. Xu, "Data-driven image color theme enhancement," *ACM Trans. Graph.*, vol. 29, no. 6, pp. 146:1–146:10, 2010.
[18] B. Wang, Y. Yu, and Y.-Q. Xu, "Example-based image color and tone style enhancement," *ACM Trans. Graph.*, vol. 30, no. 4, pp. 64:1–64:12, 2011.
[19] B.-Y. Wong, K.-T. Shih, C.-K. Liang, and H. Chen, "Single image realism assessment and recoloring by color compatibility," *IEEE Trans. Multimedia*, vol. 14, no. 3, pp. 760–769, 2012.
[20] S. Paris, P. Kornprobst, J. Tumblin, and F. Durand, "Bilateral filtering: Theory and application," in *Proc. Computer Graphics and Vision 2008*.
[21] Z. Farbman, R. Fattal, D. Lischinski, and R. Szeliski, "Edge-preserving decompositions for multi-scale tone and detail manipulation," *ACM Trans. Graph.*, vol. 27, no. 3, pp. 67–76, 2008.
[22] M. Kass and J. Solomon, "Smoothed local histogram filters," *ACM Trans. Graphics (Proc. ACM SIGGRAPH 2010)*, vol. 29, no. 4, pp. 100:1–100:10, 2010.
[23] E. S. L. Gastal and M. M. Oliveira, "Domain transform for edge-aware image and video processing," *ACM TOG*, vol. 30, no. 4, 2011, Proc. SIGGRAPH 2011, to be published.
[24] L. Xu, C. Lu, Y. Xu, and J. Jia, "Image smoothing via l0 gradient minimization," in *Proc. SIGGRAPH Asia 2011*, 2011.
[25] E. S. L. Gastal and M. M. Oliveira, "Adaptive manifolds for real-time high-dimensional filtering," *ACM Trans. Graph.*, vol. 31, no. 4, pp. 33:1–33:13, 2012.
[26] Z. Su, X. Luo, Z. Deng, Y. Liang, and Z. Ji, "Edge-preserving texture suppression filter based on joint filtering schemes," *IEEE Trans. Multimedia*, vol. 15, no. 3, pp. 535–548, 2013.
[27] Z. Su, X. Luo, and A. Artusi, "A novel image decomposition approach and its applications," *Visual Comput.*, vol. 29, no. 10, pp. 1011–1023, 2013.
[28] G. Petschnigg, R. Szeliski, M. Agrawala, M. Cohen, H. Hoppe, and K. Toyama, "Digital photography with flash and no-flash image pairs," *ACM Trans. Graph. (Proc. ACM SIGGRAPH 2004)*, vol. 23, no. 3, pp. 664–672, 2004.
[29] E. Eisemann and F. Durand, "Flash photography enhancement via intrinsic relighting," *ACM Trans. Graph.*, vol. 23, no. 3, pp. 673–678, 2004.
[30] S. Bae, S. Paris, and F. Durand, "Two-scale tone management for photographic look," *ACM Trans. Graph.*, vol. 25, pp. 637–645, 2006.
[31] K. M. He, J. Sun, and X. O. Tang, "Guided image filtering," in *Computer Vision–ECCV 2010*, vol. 6311, pp. 1–14.
[32] L. Xu, Q. Yan, Y. Xia, and J. Jia, "Structure extraction from texture via relative total variation," *ACM Trans. Graph.*, vol. 31, no. 6, pp. 139:1–139:10, 2012.
[33] R. Fattal, M. Agrawala, and S. Rusinkiewicz, "Multiscale shape and detail enhancement from multi-light image collections," *ACM Trans. Graph.*, vol. 26, 2007.
[34] Z. Farbman, R. Fattal, and D. Lischinski, "Diffusion maps for edge-aware image editing," *ACM Trans. Graph. (Proc. ACM SIGGRAPH Asia 2010)*, vol. 29, no. 6, pp. 145:1–145:10, 2010.
[35] S. Paris, S. W. Hasinoff, and J. Kautz, "Local Laplacian filters: Edge-aware image processing with a Laplacian pyramid," *ACM Trans. Graph.*, vol. 30, no. 4, pp. 1–12, 2011.
[36] C. M. Bishop, *Pattern Recognition and Machine Learning*. New York, NY, USA: Springer, 2006.
[37] F. Pitié and A. Kokaram, "The linear monge-kantorovitch linear colour mapping for example-based colour transfer," in *Proc. 4th Eur. Conf. Visual Media Production, 2007 IETCVMP*, 2007, pp. 1–9.

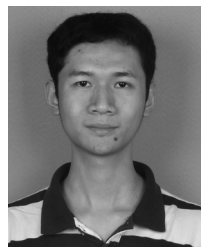

Zhuo Su (S'13) is a Ph.D. candidate of the National Engineering Research Center of Digital Life, School of Information Science and Technology, Sun Yat-sen University. He received the Master and Bachelor degree in software engineering from School of Software, Sun Yat-sen University in 2010 and 2008. His research interests include image processing and analysis, computer vision, and computer graphics.

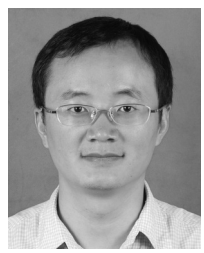

Kun Zeng received his PhD degree from Chinese Academy of Sciences in 2008. He is now an assistant professor at Sun Yat-sen University. His research interests include non-photorealistic rendering, multimedia, machine learning and computer vision.

Li Liu is currently a lecturer in Kunming University of Science and Technology, and working as a Ph.D. candidate in School of Information and Science Technology, Sun Yat-sen University, Guangzhou, China. She received her Master and Bachelor degree in computer science from Kunming University of Science and Technology in 2005 and 2002. Her research interests include computer graphics, image processing and analysis.

Bo Li received the Ph.D. degree in Mathematics from Mathematics Department, Dalian University of Technology, Dalian, in 2008. He is the Associate Professor at School of Mathematics and Information Science, Nanchang Hangkong University in China. His research interests include inverse problems in image processing and content-based image retrieval.

Xiaonan Luo is a professor of School of Information and Science Technology, Sun Yat-sen University. He is the director of National Engineering Research Center of Digital Life and the director of Digital Home Standards Committee on Interactive Applications of China Electronics Standardization Association. He won the National Science Fund for Distinguished Young Scholars granted by the National Nature Science Foundation of China. His research interests include image processing, computer graphics & CAD, mobile computing.